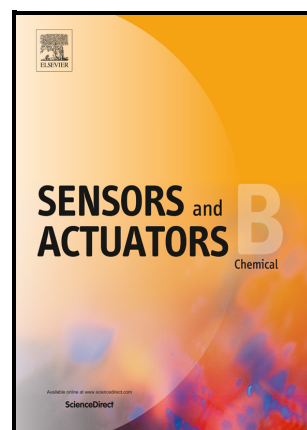


Chemoresistive NH_3 gas sensor at room temperature based on the Carbon gel- TiO_2 nanocomposites

M.D. Fernández-Ramos, L.F. Capitán-Vallvey, L.M. Pastrana-Martínez, S. Morales-Torres, F.J. Maldonado-Hódar



PII: S0925-4005(22)00745-6

DOI: <https://doi.org/10.1016/j.snb.2022.132103>

Reference: SNB132103

To appear in: *Sensors and Actuators: B. Chemical*

Received date: 5 May 2022

Revised date: 20 May 2022

Accepted date: 22 May 2022

Please cite this article as: M.D. Fernández-Ramos, L.F. Capitán-Vallvey, L.M. Pastrana-Martínez, S. Morales-Torres and F.J. Maldonado-Hódar, Chemoresistive NH_3 gas sensor at room temperature based on the Carbon gel- TiO_2 nanocomposites, *Sensors and Actuators: B. Chemical*, (2022) doi:<https://doi.org/10.1016/j.snb.2022.132103>

This is a PDF file of an article that has undergone enhancements after acceptance, such as the addition of a cover page and metadata, and formatting for readability, but it is not yet the definitive version of record. This version will undergo additional copyediting, typesetting and review before it is published in its final form, but we are providing this version to give early visibility of the article. Please note that, during the production process, errors may be discovered which could affect the content, and all legal disclaimers that apply to the journal pertain.

Chemoresistive NH₃ gas sensor at room temperature based on the Carbon gel-TiO₂ nanocomposites

M.D. Fernández-Ramos^{*a,c}, L.F. Capitán-Vallvey^{a,c}, L.M. Pastrana-Martínez^{b,c}, S. Morales-Torres^{b,c}, F.J. Maldonado-Hódar^{*b,c}.

^a *ECsens. Department of Analytical Chemistry, University of Granada, Granada 18071 (Spain).*

^b *NanoTech – Nanomaterials and Sustainable Chemical Technologies. Department of Inorganic Chemistry, University of Granada, Granada 18071 (Spain).*

^c *Unit of Excellence in Chemistry applied to Biomedicine and the Environment of the University of Granada.*

*Corresponding Author: M.D. Fernández-Ramos, *e-mail: mdframos@ugr.es and F.J. Maldonado-Hódar, * email: fjmalDON@UGR.ES*

Abstract

A resistive sensor based on films of carbon gel-TiO₂ nanocomposites prepared with different percentages of TiO₂ by a sol-gel process, was developed to determine ammonia gas. A thin film of carbon gel-TiO₂ nanocomposites dispersed in poly(vinylidene fluoride) and deposited on glass slides containing silver electrodes are used as NH₃ sensor. The resistance of the films at a potential difference of 1.0 V was determined in the presence of NH₃, CO₂, C₂H₅OH, CH₃OH, C₄H₁₀O and C₄H₈O₂ gases with concentrations in the range of 0-1000 ppm. The response of the resistive sensor expressed as response sensitivity -Response (%) - increases linearly as the gas concentration increases from 0.2 to 18.8. The sensor response is obtained at room temperature, 25°C, and under UV irradiation. The response increase with the increase of wt% of TiO₂ in the material. The sensor based on a carbon-TiO₂ nanocomposite with 50 wt% of TiO₂ presents the best performance in terms of sensitivity (sensor response ~18.8 for 100 ppm NH₃), selectivity (selectivity factor for NH₃ is about ~5.8 against C₄H₈O₂, C₄H₁₀O and ~4.5 for CO₂, CH₃OH, C₂H₅OH), stability (both long-term and short-term) and influence of humidity. Additionally, this prepared film possesses the advantages of low power consumption, cost-effectiveness and selective detection ability for NH₃ sensing.

Keywords: Resistive sensor; Carbon gel-TiO₂ nanocomposite; Ammonia gas sensor; Room temperature sensor.

1. Introduction

In recent decades, air quality and air pollution control have been the main lines of action in EU policies on environment, human health and well-being. Therefore, it is vitally important to have methods for determining gases and toxic components in the atmosphere that allow information to be obtained quickly, reliably and economically. There are also many other economic sectors where the strict control of the atmosphere composition is a key factor, such as facilities for the storage or transport of climacteric products to avoid premature ripening and the disposal of such products, among others [1]. Ammonia gas is used in a wide range of applications such as agriculture, production of fertilizers, dyes, pharmaceutical and chemistry industries. The exposure to extreme concentrations of ammonia gas might cause death, whereas low and continuous exposure could lead to various life-threatening diseases. It is of great interest to develop highly sensitive and selective sensors that could detect ammonia gas at room temperature conditions. A wide variety of gas sensors have been extensively investigated, such as electrochemical [2], catalytic pellistors [3], thermal conductivity [4], metal oxide [5] and optical gas sensors [6]. Resistive gas sensors are popular due to their reasonable price and long lifetime [7]. With this type of sensors, the changes in the electrical signal depend on the type of material (p/n-type), the physical and chemical characteristics of the analyte, such as polarity (polar/non-polar), the acid-base character, concentration and electron donor/acceptor properties. Several sensing mechanisms and phenomena such as charge transfer, a swelling effect, Schottky barrier modulation and hydrogen bonding between the sensing layer and the analyte modulate the response in resistive devices and define the performance of the gas sensor [8]. The main drawback is related to its limited selectivity and sensitivity [9]. Therefore, there is considerable interest in developing new materials and methods to obtain gas sensors with better analytical characteristics, in particular good adsorption, sensitivity, selectivity and thermodynamic stability. A wide variety of materials including metal oxides, conducting polymers, carbon materials and their composites have been used to detect toxic gases [10, 11].

Metal oxides stand out as one of the largest and most common classes of materials due to their extensive structural, physical and chemical properties for gas sensors [12, 13]. Since the working mechanism with this type of sensor is based on the interaction between the material sensor and the gas species, in most gas sensors based on metal oxide, the sensitivity response increases as the operating temperature increases, and it reaches a maximum sensitivity response at high temperature values, leading to high

power consumption. In addition, they exhibit long-term baseline drift and low selectivity for various target gases, resulting in false positive or interfering signals, and consequently limiting their versatility. It has been shown that the sensing properties are improved by modifying the structure and electronic properties by doping these metal oxides [2, 3]. Recent studies showed that metal oxide composites with trace carbon can improve the performance of the resulting material when incorporated into different types of sensors because their properties vary easily [6, 14].

Carbon-TiO₂ composites can be prepared using different synthesis procedures and combinations with a large number of carbon phases available and different loadings and using thermal treatments to fit the crystallographic TiO₂ phases [4, 5]. In addition, these composites are important functional materials with excellent physicochemical properties and have been applied in the field of catalysis [8], including photocatalysis [5], electrochemical applications in supercapacitors [10], and a sodium ion battery [11]. Nevertheless, research into the gas sensing properties of carbon-doped TiO₂ is limited. In this study, we demonstrate the successful features of resistive sensors to determination of ammonium gas based on carbon gel-TiO₂ composites.

Experimental section

1.1. Reagents and materials

(See Supplementary Material)

1.2. Preparation of carbon-TiO₂ nanocomposites

The synthesis of the carbon gel-TiO₂ nanocomposites was carried out by a sol-gel process in a three-neck balloon using a mixture of resorcinol (R)-formaldehyde (F) as the precursor of the organic fraction and TBTi as the TiO₂ precursor, adapting our previous synthesis procedure [12, 13]. Additional details are summarized in the supplementary material section.

1.3. Characterization of carbon-TiO₂ nanocomposites

The carbonized composites were characterized by combination of complementary techniques (TG-DTG, XPS, XRD, HRTEM, gases adsorption, mercury porosimetry, etc) to determine physical (porosity and surface area, morphology, crystalline phase, etc) and chemical (bulk and surface composition) properties, according to the procedures detailed in the supplementary material section.

1.4. Gas sensor fabrication

The resistive gas sensor was prepared on a clean glass slide (2.5 x 2.5 cm) by screen printing two 10 mm x 2 mm silver electrodes on it with a separation of 1.5 mm (Figure S1). Print designs were made using the pattern editor in the Adobe Illustrator software.

To prepare the sensing membranes, a solution of 61.0 mg of the PVDF polymer was prepared in 1 ml of DMA and 2 mg of carbon gel-TiO₂ powder was added, and the mixture was vigorously stirred for a few seconds. After that, 25 μ L of this cocktail was cast onto the silver electrodes in a glass support using a spin coating technique at 80 rpm for 1 min. The sensing films obtained were about 50 μ m thick.

1.5. Determination of sensor response

Figure 1 depicts the measurement system used. The experiments were performed inside a homemade plastic climate chamber (5 cm high, 7 cm wide and 14 cm long), where the sensor was introduced and connected to the electrometer (Keithley 2100 digital from Keithley Instrument GmbH, Ohio, USA). A UV lamp VL-6MC 6 W (1.4 mW/cm²) (λ = 312 nm) from Vilber (Vilber Lourmat Deutschland GmbH, Eberhardzell, Germany) was placed in the lid of the box, that has a window so that the light falls directly on the sensor, thus preventing radiation absorption by the plastic. The gas or vapour input and electrical connections are located on the side.

Figure 1

Standard mixtures of NH₃ (up to 100 ppm) or CO₂ (up to 5000 ppm) were prepared by taking variable amounts of the corresponding gas bullets and diluting them in synthetic air, controlling the gas flows which entered a mixing chamber using a computer-controlled mass flow controller (Air Liquid España S.A., Madrid, Spain) operating at a total pressure of 760 Torr and a flow rate between 100 and 500 cm³ min⁻¹. For the preparation of gas mixtures with a NH₃ up to 2 ppm a standard of 2 ppm NH₃ in nitrogen was used, with the lowest NH₃ concentration tested being 0.1 ppm. To produce different vapour concentrations from analytes liquids, from 0 to 600 ppm, and humidity conditions, from 0 to 100% RH, a Controlled Evaporator Mixer system (CEM) was used. It consists of a mass flow controller for the measurement and control of the carrier gas flow (air) and a mass flow meter for liquids (MiniCoriflow) with a range of 0.4–20 g·h⁻¹ of liquid. A 3-way EMC mixing valve and an evaporator controls the liquid flow and liquid mixing with the carrier gas flow. In addition, it contains a temperature-controlled heat exchanger to heat the mixture and completely evaporate the liquid (100

°C for water; 77.1 °C for ethyl acetate; 78 °C for ethanol; 65°C for methanol; 118 °C for butanol).

The measurements were repeated three times to check for experimental error. The current through the sensing film was measured with a constant 1.0 V potential difference applied to the electrodes, with a good ohmic contact between the silver electrodes and the sensing film.

To study the gas sensitivity of the carbon gel-TiO₂ nanocomposite films, different gases and vapours were studied, namely ethanol, methanol, 1-butanol, ethyl acetate, ammonia and carbon dioxide. Measurements were performed as follows: initially, the resistance value of the nanocomposite film was measured under synthetic air, then a gas or vapor of known concentration was passed into the climatic chamber for 2 minutes, and then the resistance value was measured. The nanocomposite film is then removed from the climatic chamber for 2 minutes and then the cycle is repeated. All the experiments were performed at room temperature (25 °C ± 2 °C) with a relative humidity of 55 ± 2%, with ambient pressure and UV lighting.

The response sensitivity, Response, is defined as:

$$Response = \frac{R_g - R_a}{R_a} \times 100 (\%) \quad (\text{eq.1})$$

with R_a being the resistance of the sensor under UV lighting, in synthetic air and R_g the resistance of the sensor in the presence of the tested gases. In all cases, the response sensitivity increases as the concentration of the gas or vapour increases.

The response time is defined as the time it takes for the sensor film to reach 90% of the maximum sensitivity value in the presence of the target gas (t_{90}), while the time it takes for the sensor to recover 10% of the initial sensitivity response value is referred to as the recovery time (t_{10}).

Selectivity is the relative response between different gases compared to the reference gas. The selectivity is the ability of the sensor to discriminate the gas of interest when this is present together with similar ones. The selectivity can be defined by the interference ratio K as:

$$K = \frac{S_A}{S_B} \quad (\text{eq. 2})$$

where S_A and S_B are the responses of a sensor for the target gas and an interfering gas respectively, for equivalent concentrations [15].

2. Results and discussion

Four RF polymer-TiO₂ composites were prepared with a theoretical content in TiO₂ of 10, 20, 30 and 50 wt%. During pyrolysis, composites undergo a weight loss (WL). The WL is mainly associated with the transformation of the organic RF-polymer into a carbon gel, which can be analysed in three phases [16], corresponding to the peaks observed in the DTG profile (Figure S2). Surface compositions were analysed by XPS and the results are summarized in Table S1. There is a good correlation between the total TiO₂ content and the atomic Ti content on the surface, which denotes a homogeneous distribution of the TiO₂ phase in the composite. The binding energy (BE) determined for the Ti 2p_{3/2} region is always between 459.1 - 459.3 eV, corresponding to the Ti⁴⁺ species. The O/Ti atomic ratio is always greater than 2 because of the contribution of the oxygen surface groups (OSG) linked to the carbon phase (C-O and C=O) remaining from the crosslinked RF polymeric structure. Details of the chemical transformations during carbonization are given in the supplementary material section. The morphology of the samples was analysed by HRSEM (Figure 2A). Large, dense and compact particles are observed, in general, coated by another structured phase as a 3D network of almost spherical particles that coalesce to form a porous structure. This is the typical coral-like nanostructure previously described for RF carbon gels [17]. Mapping obtained by HRTEM (Figure 2B) confirms that very small and homogeneously distributed TiO₂ nanoparticles are observed at intermediate TiO₂ loading (Figure 2Bb).

Figure 2

A detailed analysis showed TiO₂ nanoparticles with a size typically below 4-5 nm, but clearly crystalline as indicated by the ordered layers inside the nanocrystals. The interlayer distance is around 3.5 Å for most TiO₂ nanoparticles, which corresponds to the (101) crystallographic planes of anatase. Sintering and particle size increased at higher TiO₂ content (Figure 2Bc). In this case, although most of the TiO₂ nanoparticles stay small, some of them clearly exceed 20-30 nm in diameter and are responsible for the XRD peaks detected in this sample. Moreover, analysing the interlayer distances, together with the results discussed above for anatase particles, these large particles showed an interlayer distance of about 3.2 Å, corresponding to the (110) crystallographic planes of rutile. Thus, sintering and phase transformation (anatase to rutile) seem to occur simultaneously and probably in particles formed in an environment

poor in carbon or clearly segregated from the composite due to the high TiO₂ content of this sample.

The porous characterization of carbonized composites was carried out by combining the analysis of the open porosity (large mesopores and macropores) and the narrow microporosity determined by mercury porosimetry and physical adsorption of CO₂, respectively. The results are summarized in Table S1, and the corresponding PSD determined by mercury porosimetry is shown in Figure S3 (see the supplementary material section). The crystallographic analysis of these nanoparticles was carried out by XRD (Figure S4). The assignment of the XRD peaks was carried out according to the JCPDS files and the bibliography [18]. The absence of diffraction peaks in the XRD patterns due to the TiO₂ phases is noteworthy for the composites with TiO₂ content less than 54% (30Ti). Only in the case of 50Ti, with 84% TiO₂, was a mixture of anatase and rutile detected (see supplementary material section).

2.1. Gas sensing performance of carbon gel-TiO₂ nanocomposites

Before determining the performance of the sensing films against the different gases, the electrical resistance of the composites was determined in both dark and UV-irradiation conditions, in order to elucidate the influence of each phase on this parameter. The results are presented in Table S2. Clearly, the carbon phase presents the highest electrical resistance, both in the dark and under UV-irradiation. TiO₂ and P25 show resistance values in the same order of magnitude. In all cases, the resistance decreases under UV-irradiation because of the photo-excited electrons generated, therefore this effect is stronger as the TiO₂ content increases (R values decrease under UV between 5 to 20% from 10Ti to 50Ti). Thus, the changes in the performance of the sensors must be related to the modifications in the concentration and properties of TiO₂ throughout the different composites.

In order to achieve the best sensing response, the sensor design was optimized. For this, four sensors based on silver electrodes with different width values were prepared – 1, 2, 3 and 4 mm – and each sensor was exposed to an ammonia stream of 10 ppm. The 1-mm sensor was discarded since its small diameter makes it difficult to carry out the electrical connection and consequently, make a reliable measurement. After 2 min of contact with the gas, the response sensitivity obtained for the 2-, 3- and 4-mm wide sensors were 8.2 and 8.0% and 8.1 %, respectively. 2 mm was selected as the optimal value since there is no significant difference when the size is increased.

The amount of material deposited on the sensor varied from 0.5 mg to 5 mg of 50Ti and the corresponding sensor films were also exposed to an ammonia stream of 10 ppm for 2 min. No response was obtained with the sensor with 0.5 mg of 50Ti, and the response sensitivity with the sensor containing 1, 2, 3 and 5 mg of 50Ti % was 3.0, 8.0, 8.4 and 8.3 %, respectively. Thus, when the amount of the material increased above 2 mg, no improvement in sensitivity was observed, and 2 mg of sample was selected as the optimal value for later experiments.

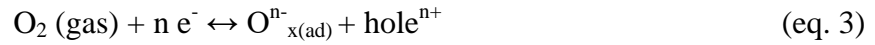
To check the gas-sensing capability, different sensors were made with different compositions of the sensing material (i.e., 10Ti, 20Ti, 30Ti and 50Ti) in the optimal conditions described above. Sensitivity and response time are known to improve with a reduction in particle size, microstructural changes and alterations in electronic properties on the surface of the material [7].

The effect of physicochemical changes on the interaction with different gases had to be analysed individually. The sensors were exposed to atmospheres of different gases and vapours such as ammonia, carbon dioxide, ethanol, methanol, butanol and ethyl acetate, and the response was recorded after 2 min of exposure. The results are shown in Figure S5. It is observed that the sensitivity increases as the percentage of TiO₂ in the sensor increases, increasing the slope of the corresponding dependence. The linear range of application of each sensor was: ammonia up to 100 ppm; carbon dioxide up to 1000 ppm; ethanol up to 300 ppm; ethyl acetate up to 675 ppm; methanol up to 250 ppm; and butanol up to 500 ppm, with a good linear fit ($R^2 > 0.9798$) for all gases tested see Table 2. (Figure 3). In the case of methanol, when the 10Ti sensor was used, no response was obtained until a value of 100 ppm of methanol was reached. It is known from previous studies that trace carbon doping has a certain influence on gas response [19]. Although the best gas response for carbon dioxide and ethyl acetate was obtained with 30Ti, for alcohols (C₁, C₂, C₄), the best performance is achieved with 50Ti, establishing that this is the appropriate range of carbon doping, with relatively moderate electrical conductivity and the largest specific surface area producing the best gas sensing performance.

Figure 3

An increase in the percentage of TiO₂ in the composite decreases the resistance (Table 1), accelerating the speed of transfer of electrons on the surface of the material, increasing the specific surface area and, therefore, the response (%) to gas (Figure 4). Concerning the behaviour of the sensor, it is observed that when the sensor is in

ambient conditions, the principal component of the atmosphere able to interact with the photogenerated electrons is oxygen. The possible sensing mechanism of the oxygen with the sensor is as follows:



For oxygen adsorption on the grain surface, a space-charge layer of appropriate characteristics is formed, and the conductivity of the material depends essentially on the mobility of the electrons inside the grains. For any gas present in the atmosphere, oxidizing or reducing gas molecules interact with the sensing material causing its conductivity to increase or decrease [20]. Thus, the physicochemical properties of the composites, such as composition, crystal size and crystallographic forms, distribution and dispersion of TiO₂ nanoparticles, degree of imperfections determine the mobility of the electrons in the material and therefore, the electrical resistance. As the size of the crystal increases, the path followed by the electrons to reach the surface of the crystal increases and, consequently, the probability of the electron-hole recombination, thus increasing the resistance of the material.

As demonstrated by XRD/HRTEM, the particle size of TiO₂ does not increase significantly up to a TiO₂ content of 84% (sample 50Ti). The variation of the resistance of materials in air under UV radiation with respect to dark conditions decreases linearly with the TiO₂ content (Figure S6) for samples 10Ti, 20 and 30Ti, but it is maintained or even slowly increases for 50Ti, since the sintering in this sample hinders the generation of electrons and their mobility.

Exposure of the resistive sensor to oxidizing gases or electron acceptors decreases the resistance value when the concentration of this gas increases, as is the case with carbon dioxide:



When the sensor is exposed to increasing concentration values of an electron donor or reducing gases, the value of the resistance increases. This happens when the sensor is exposed to atmospheres of ethanol, methanol, butanol, ethyl acetate or ammonia. The basic theory behind gas sensing lies in its connection with band theory: p-type oxides show a resistance increase in the presence of traces of reducing gases, and a resistance decrease to oxidizing gases, and n-type oxides show the opposite behaviour. In our experimental conditions, the materials behave like an n-type semiconductor.

It is known that light activation can speed up the desorption of absorbed gases, which greatly reduces the response/ recovery time [21]. Under UV illumination, the amounts

of residual O_2 adsorbed on the surface of the sensor increases, so the significant reduction of those amounts by photocatalytic reaction results in an increase in the photocurrent, with a decrease in the resistance.

To evaluate the possibility of using the gas sensor in real applications, an analytical characterization was made. The limit of detection (LOD) was calculated as usual by using $LOD = t_0 + 3s_0$, where t_0 is the average blank signal and s_0 is the critical level or standard deviation of the blank, which is determined from eight replicas for each of the gases tested.

The precision as the short-term (repeatability) and long-term (reproducibility) stability of the sensors was checked to determine the surface poisoning effect. The short-term stability was confirmed by recording the repeating gas sensing measurements for specific gas at least three times under the same experimental conditions. To check the repeatability, the 50Ti-doped carbon sensor was exposed to an atmosphere of 10 ppm NH_3 and after reaching a stable signal, it was exposed to air for 2 min to recover the initial signal. Figure 4a shows the alternation of five cycles between both atmospheres with a repeatability of 0.3%. It is observed that the resistance increases in the presence of NH_3 (electron acceptor) and that the sensor maintains its initial resistance in air.

The role that UV light exerts on the desorption of the gas retained in the material is like that produced by the increase in temperature, where the photoexcitation or thermal activation, as in our case, returns the electrons of the analyte with photo generated holes and the analytes are desorbed. The recombination of the analytes with photogenerated holes also enables the desorption of the analytes. Consequently, the fast adsorption of the analytes can be explained by the “cleaned” surface of the carbon gel- TiO_2 material due to the removal of O_2^- upon UV illumination [22]. The response time (t_{90}) and recovery time (t_{10}) for the gases tested with carbon doped TiO_2 50% film for 10 ppm NH_3 and 300 ppm of the rest of the gases are shown in Table 4. In the case of NH_3 , the response time and recovery time is slightly higher than for the other gases tested. The low response and recovery time of these sensors, in the order of a few seconds, are due to the UV illumination facilitating the desorption of analytes.

The long-term stability was confirmed by the sensor test with a specific time interval during which the sensors were kept in an open-air environment. Long-term stability was studied by measuring the response of the sensor when it is exposed to 50 ppm NH_3 for 150 days from a set of sensors using a Shewhart diagram. We defined a long-term sensor (T1) as one in which the signal for a constant concentration of NH_3 remains

within the control line on the Shewhart chart. In addition, we defined the long-term T2 as the time during which the sensor responds to NH₃, although it must be recalibrated. Figure 6b shows the control chart for the sensor; after 150 days, the sensor signal remains within the established control limits. The sensor possesses excellent long-term stability during the period tested, which suggests significant durability.

Selectivity is an important aspect of the gas-sensing performance. The selectivity of our sensor was studied for 100 ppm of all the gases tested, taking NH₃ as the target gas and the other gases tested as interfering gases, using eq. 2 (Figure 4c). As observed, the sensor response was ~18.8 for 100 ppm NH₃. The selectivity factor for 100 ppm NH₃ is about ~5.8 against C₄H₈O₂ and C₄H₁₀O and ~4.5 for CO₂, CH₃OH and C₂H₅OH, the response for NH₃ the response is of the order of three and four times higher than for the rest of the gases tested, demonstrating that it is possible to selectively determine ammonia.

It is known that relative humidity (% RH) is an important factor that affects the sensing performance of the sensor [23]. Generally speaking, the sensor response increases with an increasing % RH because gas dissolves in water adsorbed on the surface of carbon-doped nanomaterials, producing a competitive sorption of gas and water molecules on the surface of the active layer. The effect of %RH on the response of the XTi sensor at ambient temperature (25°C) is shown in Figure 6d, with no influence observed for 10Ti, while for the rest of materials the influence is less than 2.0%. Only when the %RH is greater than 85% there is any influence on the signal. There is a clear effect of the composite composition on the influence of %RH; thus, the low influence of %RH on the response of the 10Ti sample is related to the high C-content and consequently, to the hydrophobic character of this sample. The influence of RH for the other samples increased as the TiO₂ content increased, and it depends on the RH%; thus below 40%, the response of the sensors varies as 10Ti < 20Ti < 30Ti < 50Ti, but at higher values of %RH, the opposite behaviour is observed (20Ti > 30Ti > 50Ti). Thus, the slope of the lines in Figure 4d is higher for samples with an intermediate content of both phases and, therefore, intermediate hydrophilicity. The results show that the carbon gel-TiO₂ nanoparticle gas sensor has good moisture stability. All experiments were carried out at room temperature (25 °C ± 2 °C).

Table 2

Table 3 summarizes the principal analytical performance characteristics of resistive sensors based on carbon doped with TiO₂ reported in the literature. Our proposed sensor

makes it possible to determine gases at ambient temperature with a good selectivity, particularly to NH_3 gas. The response and recovery times are comparably better than those found in the literature, probably due to the illumination of the sensor with UV light.

Table 3

3. Conclusions

Carbon gel- TiO_2 nanocomposites have been proposed as sensing materials. The C- XTiO_2 exhibits different gas sensing to ammonia, ethanol, methanol, butanol, ethyl acetate and carbon dioxide at ambient temperature and under UV illumination.

The resistive sensor behaves like an n-type semiconductor. Carbon doped with 84% TiO_2 has the best sensor properties: good selectivity towards ammonia (100 ppm, $S = 18$), low response and recovery times (50 and 170 s, respectively), stability over time and a low influence of humidity on the response with a low applied voltage of 1.0 V. These good results, together with the low price of carbon, make sensors based on carbon doped with TiO_2 excellent candidates for the development of low-priced commercial resistive sensors for the selective monitoring of specific gas analytes.

CRedit authorship contribution statement

M.D. Fernández-Ramos: Conceptualization, Investigation, Validation, Formal analysis, Writing, original draft, Writing, review and editing. **L.F. Capitan-Vallvey:** Validation, Writing, original draft, Resources, Writing, review and editing sources. **L.M. Pastrana-Martínez:** Synthesis, Characterization, Formal analysis, Resources, Writing, original draft, Writing, review and editing. **S. Morales-Torres:** Synthesis, Resources, Characterization, Formal analysis, Writing, original draft, Writing, review and editing. **F.J. Maldonado Hódar:** Conceptualization, Resources, Writing, original draft, Writing, review and editing, Funding acquisition, Supervision.

Declaration of Competing Interest

The authors declare that they have no known competing financial interests or personal relationships that would influence the work reported in this paper.

Acknowledgements

This work was financially supported by the PCI2020-112045 project from MCIN/AEI/10.13039/501100011033 and European Union Next GenerationEU/PRTR, as part of the PRIMA Programme (Nano4Fresh project). It received additional funding

from the Spanish Ministry of Economy and Competitiveness (Project PID2019-103938RB-I00) and the Junta de Andalucía (Projects B-FQM-243-UGR18 and P18-RT-2961).

Table 1. Influence of UV light on the resistance value of different materials in air.

Material	Electrical Resistance (k Ω)	
	Dark (without UV)	UV
C	34228.3 \pm 32.5	32725.0 \pm 36.3
TiO ₂	90.7 \pm 17.2	85.2 \pm 12.4
P25	119.1 \pm 8.2	100.4 \pm 6.2
10Ti	25540.0 \pm 22.1	24021.3 \pm 18.3
20Ti	9236.3 \pm 7.3	8205.1 \pm 8.2
30Ti	5432.6 \pm 6.5	4302.1 \pm 7.2
50Ti	528.7 \pm 4.6	430.2 \pm 3.8

Analytical Parameter	Gases					
	NH ₃	C ₂ H ₅ OH	CH ₃ OH	C ₄ H ₁₀ O	C ₄ H ₈ O ₂	CO ₂
Slope (b)	0.33 \pm 0.029	0.034 \pm 0.0004	0.04 \pm 0.004	0.010 \pm 0.004	0.012 \pm 0.001	0.005 \pm 0.001
Intercept (a)	1.12 \pm 0.058	0.86 \pm 0.014	0.26 \pm 0.022	1.145 \pm 0.018	2.057 \pm 0.018	3.69 \pm 0.020
R ²	0.9750	0.9874	0.9950	0.9934	0.9798	0.9947
LOD (ppm)	1.55	2.55	2.62	48.00	46.75	15.60
LQD (ppm)	5.20	8.52	8.75	162.00	155.83	52.10
Response time t ₉₀	50	20	25	32	30	28
Recovery time t ₁₀	170	60	58	65	68	62

Table 2. Analytical characteristics of sensing membrane 50Ti for all gases tested.

Table 3. A comparison of the performance of resistive sensors based on C-XTiO₂ in the detection of different gases.

Material	Synthesis	Gas	[Gas] ppm	Response time (s)	Recovery time (s)	Phase	TiO ₂ size (mm)	Sensor response	T (°C)	Ref.
C-Ti	Sol-gel	NO ₂	10	240	1044	-	8.8	R _g /R _a	Room T.	[24]
C-Ti nano composite	Sol-gel	NO ₂	1-100	-	-	p-type	-	(R ₀ -R _{gas})/R ₀ x100	50-200	[25]
C-Ti nano tubes array	Chem. Thermal.	H ₂	5000	-	-	-	-	current	100	[26]

C-xTi	Solvothermal-calc.	Pentanol	100	100	675	-	30	R _a /R _g	170	[19]
C-xTi	Sol-gel	NH ₃	0-100	50	170	n-type	-	(R _g -R _a)/R _{ax} 100	Room T.	Current Study

References

- [1] V. Paul, R. Pandey, Role of internal atmosphere on fruit ripening and storability--a review, *Journal of Food Science and Technology*, 51(2014) 1223-50.
- [2] M. Mabrook, P. Hawkins, A rapidly-responding sensor for benzene, methanol and ethanol vapours based on films of titanium dioxide dispersed in a polymer operating at room temperature, *Sensors and Actuators B: Chemical*, 75(2001) 197-202.
- [3] Z. Yang, L. Jiang, J. Wang, F. Liu, J. He, A. Liu, et al., Flexible resistive NO₂ gas sensor of three-dimensional crumpled MXene Ti₃C₂T_x/ZnO spheres for room temperature application, *Sensors and Actuators B: Chemical*, 326(2021) 128828.
- [4] H. Hamad, J. Castelo-Quibén, S. Morales-Torres, F. Carrasco-Marín, A.F. Pérez-Cadenas, F.J. Maldonado-Hódar, On the Interactions and Synergism between Phases of Carbon-Phosphorus-Titanium Composites Synthetized from Cellulose for the Removal of the Orange-G Dye, *Materials (Basel)*, 11(2018) 1766.
- [5] L.M. Pastrana-Martínez, S. Morales-Torres, S.A.C. Carabineiro, J.G. Buijnsters, J.L. Figueiredo, A.M.T. Silva, et al., Photocatalytic activity of functionalized nanodiamond-TiO₂ composites towards water pollutants degradation under UV/Vis irradiation, *Applied Surface Science*, 458(2018) 839-48.
- [6] A. Dankeaw, G. Pongchan, M. Panapoy, B. Ksapabutr, In-situ one-step method for fabricating three-dimensional grass-like carbon-doped ZrO₂ films for room temperature alcohol and acetone sensors, *Sensors and Actuators B: Chemical*, 242(2017) 202-14.
- [7] E.A. Nunes Simonetti, T. Cardoso de Oliveira, Á. Enrico do Carmo Machado, A.A. Coutinho Silva, A. Silva dos Santos, L. de Simone Cividanes, TiO₂ as a gas sensor: The novel carbon structures and noble metals as new elements for enhancing sensitivity – A review, *Ceramics International*, 47(2021) 17844-76.
- [8] E. Bailón, F. Carrasco-Marín, A. Perez-Cadenas, F.J. Maldonado-Hódar, Chemoselective Pt-catalysts supported on carbon-TiO₂ composites for the direct hydrogenation of citral to unsaturated alcohols, *Journal of Catalysis*, 344(2016).
- [9] J. Smulko, M. Trawka, Gas selectivity enhancement by sampling-and-hold method in resistive gas sensors, *Sensors and Actuators B: Chemical*, 219(2015) 17-21.
- [10] A. Elmouwahidi, E. Bailón-García, J. Castelo-Quibén, A.F. Pérez-Cadenas, F.J. Maldonado-Hódar, F. Carrasco-Marín, Carbon-TiO₂ composites as high-performance supercapacitor electrodes: synergistic effect between carbon and metal oxide phases, *Journal of Materials Chemistry A*, 6(2018) 633-44.
- [11] Y. Ge, H. Jiang, J. Zhu, Y. Lu, C. Chen, Y. Hu, et al., High cyclability of carbon-coated TiO₂ nanoparticles as anode for sodium-ion batteries, *Electrochimica Acta*, 157(2015) 142-8.
- [12] F.J. Maldonado-Hódar, C. Moreno-Castilla, J. Rivera-Utrilla, Synthesis, pore texture and surface acid-base character of TiO₂/carbon composite xerogels and aerogels and their carbonized derivatives, *Applied Catalysis A: General*, 203(2000) 151-9.
- [13] C. Moreno-Castilla, F.J. Maldonado-Hódar, Synthesis and surface characteristics of silica- and alumina-carbon composite xerogels, *Physical Chemistry Chemical Physics*, 2(2000) 4818-22.

- [14] E.A. Nunes Simonetti, T. Cardoso de Oliveira, Á. Enrico do Carmo Machado, A.A. Coutinho Silva, A. Silva dos Santos, L. de Simone Cividanés, TiO₂ as a gas sensor: The novel carbon structures and noble metals as new elements for enhancing sensitivity. A review, *Ceramics International*, 47 (2021) 17844-76.
- [15] B.T. Raut, M.A. Chougule, S.R. Nalage, D.S. Dalavi, S. Mali, P.S. Patil, et al., CSA doped polyaniline/CdS organic–inorganic nanohybrid: Physical and gas sensing properties, *Ceramics International*, 38(2012) 5501-6.
- [16] F.J. Maldonado-Hódar, M.A. Ferro-García, J. Rivera-Utrilla, C. Moreno-Castilla, Synthesis and textural characteristics of organic aerogels, transition-metal-containing organic aerogels and their carbonized derivatives, *Carbon*, 37(1999) 1199-205.
- [17] S.A. Al-Muhtaseb, J.A. Ritter, Preparation and Properties of Resorcinol–Formaldehyde Organic and Carbon Gels, *Advanced Materials*, 15(2003) 101-14.
- [18] N. Khatun, Anita, P. Rajput, D. Bhattacharya, S.N. Jha, S. Biring, et al., Anatase to rutile phase transition promoted by vanadium substitution in TiO₂: A structural, vibrational and optoelectronic study, *Ceramics International*, 43(2017) 14128-34.
- [19] D. Zhao, X. Zhang, L. Sui, W. Wang, X. Zhou, X. Cheng, et al., C-doped TiO₂ nanoparticles to detect alcohols with different carbon chains and their sensing mechanism analysis, *Sensors and Actuators B: Chemical*, 312(2020) 127942.
- [20] D.E. Williams, Semiconducting oxides as gas-sensitive resistors, *Sensors and Actuators B: Chemical*, 57(1999) 1-16.
- [21] H. Chen, Y. Liu, C. Xie, J. Wu, D. Zeng, Y. Liao, A comparative study on UV light activated porous TiO₂ and ZnO film sensors for gas sensing at room temperature, *Ceramics International*, 38(2012) 503-9.
- [22] K. Anothainart, M. Burgmair, A. Karthigeyan, M. Zimmer, I. Eisele, Light enhanced NO₂ gas sensing with tin oxide at room temperature: conductance and work function measurements, *Sensors and Actuators B: Chemical*, 93(2003) 580-4.
- [23] G.J. Thangamani, S.K.K. Pasha, Titanium dioxide (TiO₂) nanoparticles reinforced polyvinyl formal (PVF) nanocomposites as chemiresistive gas sensor for sulfur dioxide (SO₂) monitoring, *Chemosphere*, 275(2021) 129960.
- [24] M. Wang, C. Jin, Q. Luo, E.J. Kim, Sol-gel derived TiO₂–carbon composites with adsorption-enhanced photocatalytic activity and gas sensing performance, *Ceramics International*, 46(2020) 18608-13.
- [25] W.-J. Liou, H.-M. Lin, Nanohybrid TiO₂/carbon black sensor for NO₂ gas, *China Particuology*, 5(2007) 225-9.
- [26] N. Kılınc, E. Şennik, M. Işık, A.Ş. Ahsen, O. Öztürk, Z.Z. Öztürk, Fabrication and gas sensing properties of C-doped and un-doped TiO₂ nanotubes, *Ceramics International*, 40(2014) 109-15.

Authors Biographies

M.D. Fernández-Ramos

M.D. Fernández-Ramos received B.Sc. and Ph.D. degrees in Chemistry from University of Granada, Granada, Spain, in 1993 and 1997, respectively. She is currently an Associate Professor in the Department of Analytical Chemistry of Granada (Spain). She has authored nearly 62 peer-reviewed scientific papers, 5 book chapters, and holds 4 patents. Her current research interest include the design, development and fabrication of sensors and portable instrumentation for environmental, health and food analysis. She has special interest in gas sensors and capillary-based microfluidic devices.

L.F. Capitán-Vallvey

L.F. Capitán-Vallvey received B. Sc. And Ph. D. degrees in Chemistry from Faculty of Sciences, University of Granada, Granada, Spain in 1973 and 1986, respectively. In

1983, he founded the Solid Phase Spectrometry Group (SPSG) and in 2000, together with Prof. Palma-López, the interdisciplinary group ECsens, which includes chemists, physicists and electrical and computer engineers at the University of Granada. He is currently a Full Professor of analytical chemistry at the University of Granada. He has authored nearly 370 peer-reviewed scientific papers, 6 books, and 25 book chapters, and holds 6 patents. His current research interest are the design, development and fabrication of sensors and portable instrumentation for environmental, health and food analysis and monitoring. Recently, he has been interested in printing chemical sensors and capillary-based microfluidic devices.

L. M. Pastrana-Martínez

L.M. Pastrana-Martínez is Ph.D. (Environmental Chemistry – 2010). She joined at the Faculty of Engineering, University of Porto (FEUP), Portugal from 2010 to 2017. Since January 2018, she has held the Ramón y Cajal position at the University of Granada, Spain. Her main research interests are focused in environmentally friendly technologies for management and treatment of air and water, particularly in the application of adsorption and solar advanced oxidation processes using nano- and macro-structured materials. Ongoing research includes the preparation, characterization and design of catalysts (tailored carbon-based materials, MOFs and semiconductor materials) for high-efficient (photo- and electro-) catalytic technologies for wastewater and air treatment.

S. Morales-Torres

S. Morales Torres is Associate Researcher at Faculty of Sciences of University of Granada (Spain) since 2017. He obtained his PhD degree by UGR in 2009 and then, he did a postdoctoral stage at Faculty of Engineering - University of Porto (FEUP, Portugal) for 7 years. His research interest involves the development of carbon materials, catalysts and membranes for energy and environmental applications. To date, he co-authored a patent and 63 articles in international JCR journals. He acted as guest Editor of 5 special issues of international scientific journals and is involved in the supervision of PhD and undergraduate students.

F.J. Maldonado-Hódar

F.J. Maldonado-Hódar is Full Professor at the University of Granada (Department of Inorganic Chemistry) since 2012 with docent activities in various degrees, Doctorate and Master Programs, as well Specialization Courses in the field of Heterogeneous Catalysis and Material Sciences. His research is focused on the design of advanced nanomaterials and the study of their applications through adsorption and catalysis for the production of clean energy, valuable products from fine chemistry or environmental processes for the air and water protection. Is co-author of 6 International patents, more than 160 publications cited around 6300 times ($h = 40$), 8 books chapters, more than 200 communications in International Congresses.

Credit authorship contribution statement

M.D. Fernández-Ramos: Conceptualization, Investigation, Validation, Formal analysis, Writing, original draft, Writing, review and editing. **L.F. Capitan-Vallvey:** Validation, Writing, original draft, Resources, Writing, review and editing sources. **L.M. Pastrana-Martínez:** Synthesis, Characterization, Formal analysis, Resources, Writing, original draft, Writing, review and editing. **S. Morales-Torres:** Synthesis,

Resources, Characterization, Formal analysis, Writing, original draft, Writing, review and editing. **F.J. Maldonado Hódar**: Conceptualization, Resources, Writing, original draft, Writing, review and editing, Funding acquisition, Supervision.

Declaration of Interest statement

The authors declare that they have no known competing financial interests or personal relationships that would influence the work reported in this paper.

Figure captions

Figure 1. Schematic diagram for the homemade gas sensor testing system.

Figure 2. A: HRSEM images showing the morphology of carbon gel–TiO₂ composites; B: HRTEM and mapping images of (a, b) 20Ti and (c, d) 50Ti (measurements correspond to 10 interlayer distances).

Figure 3. Response (%), sensitive response, of sensors prepared with the different carbon gel-XTiO₂ composites against selected gases.

Figure 4.a): Response and recovery curves of composite 50Ti at 10 ppm NH₃; b): Shewhart control chart for check long-term stability of the sensor; c): Selectivity of 50Ti for 100 ppm of gases.; d): Humidity influence on XTi sensing membranes. All experiments were carried out at room temperature (20 °C).

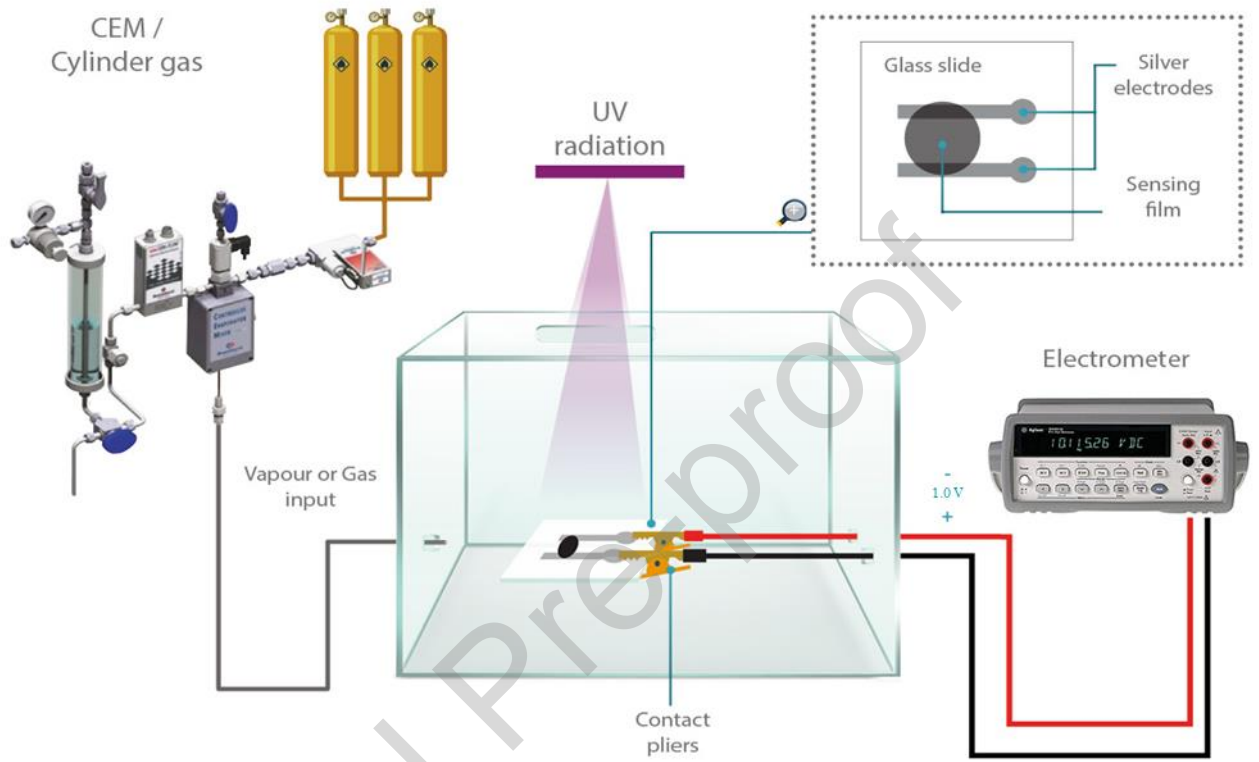


Figure 1

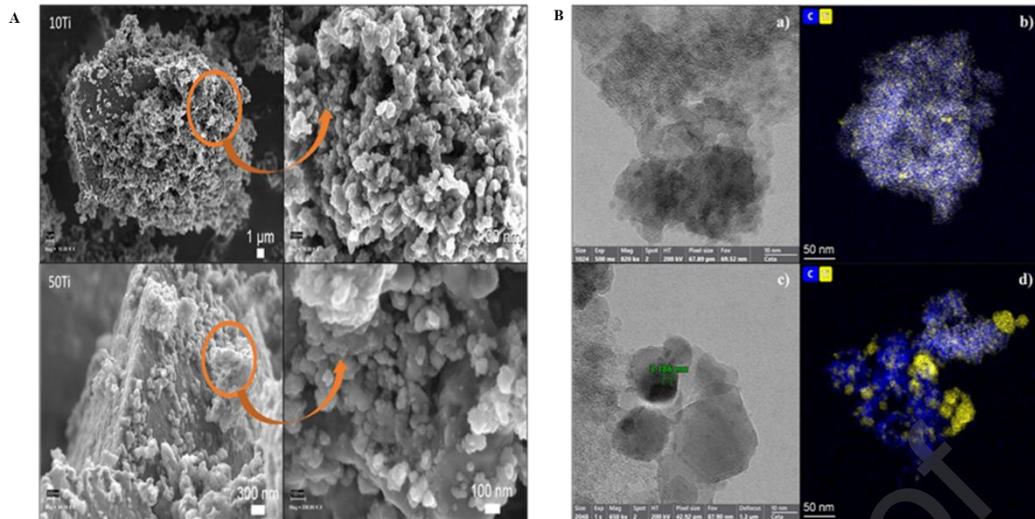


Figure 2

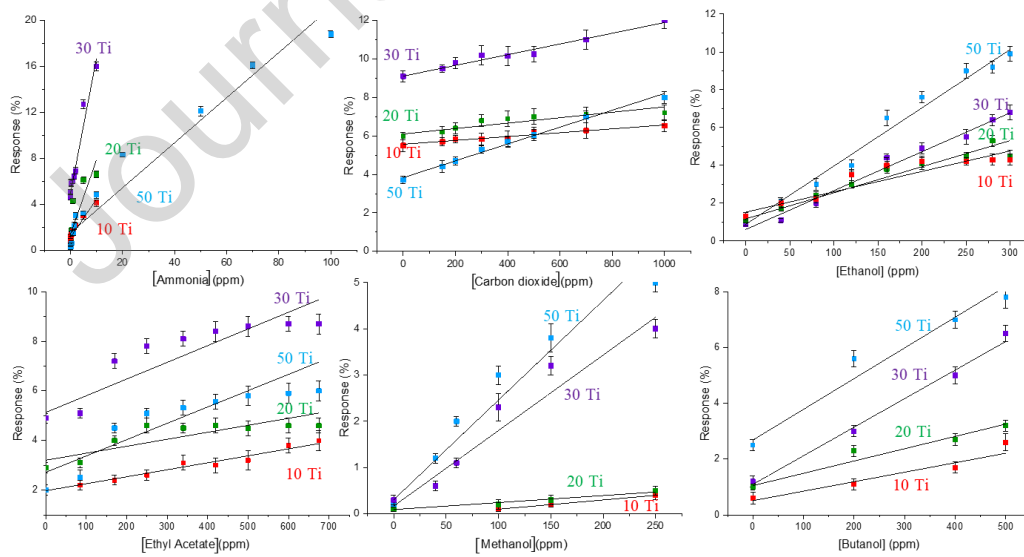


Figure 3

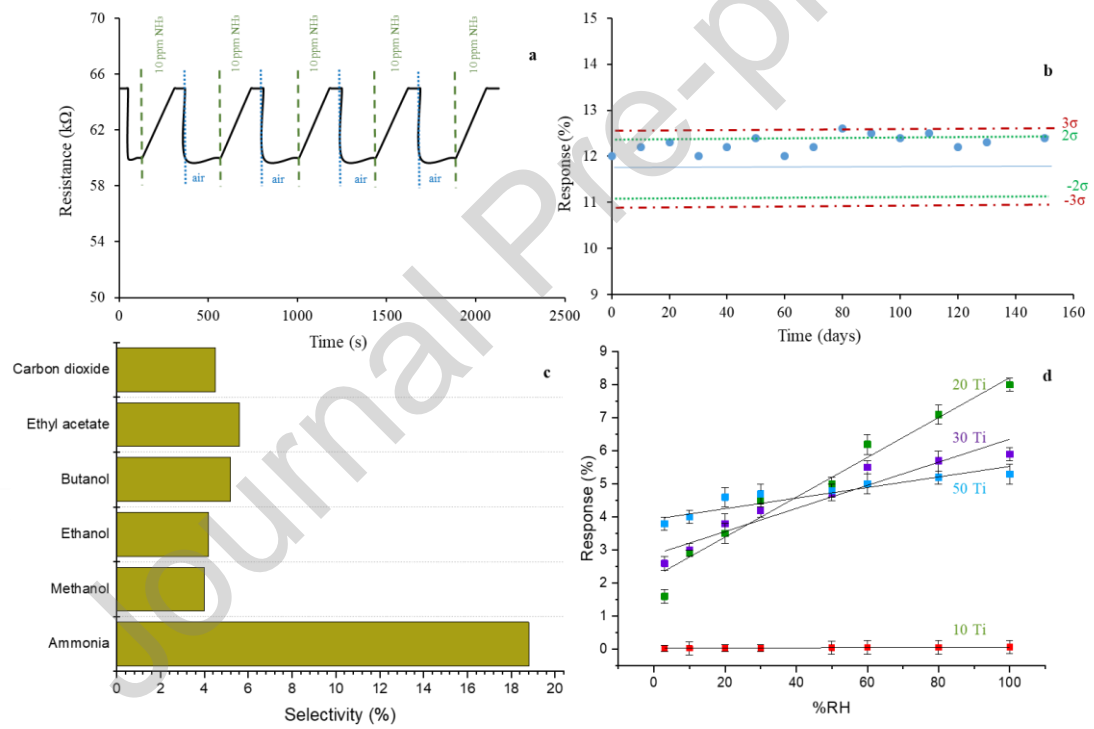
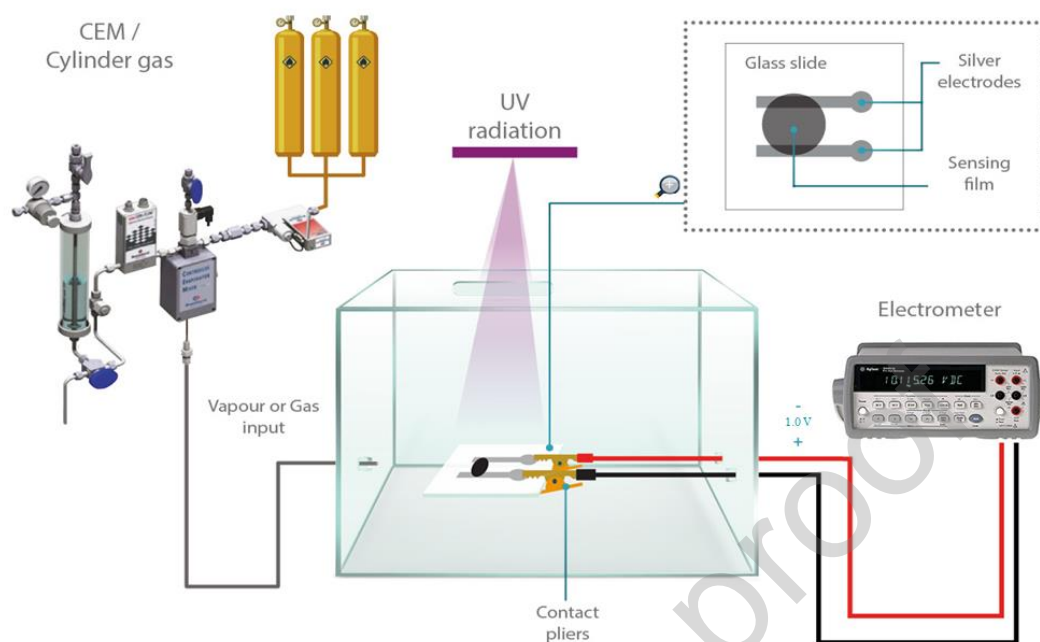


Figure 4

Graphical abstract



Highlights

- A resistive sensor gas based on films of carbon gel-TiO₂ nanocomposites with different percentage of TiO₂ was developed
- The C-XTiO₂ exhibit different gases sensing at ambient temperature and under UV illumination.
- Carbon doped with 84% TiO₂ possess the best sensing properties for selective ammonia determination.
- The C-XTiO₂ as resistive gas sensor possesses: low power consumption, cost-effective and detection ability for NH₃ sensing.

Table 1. Influence of UV light on the resistance value of different materials in air.

Material	Electrical Resistance (kΩ)	
	Dark (without UV)	UV
C	34228.3 ± 32.5	32725.0 ± 36.3
TiO ₂	90.7 ± 17.2	85.2 ± 12.4
P25	119.1 ± 8.2	100.4 ± 6.2
10Ti	25540.0 ± 22.1	24021.3 ± 18.3

20Ti	9236.3 ± 7.3	8205.1 ± 8.2
30Ti	5432.6 ± 6.5	4302.1 ± 7.2
50Ti	528.7 ± 4.6	430.2 ± 3.8

Table 2. Analytical characteristics of sensing membrane 50Ti for all gases tested.

Analytical Parameter	Gases					
	NH ₃	C ₂ H ₅ OH	CH ₃ OH	C ₄ H ₁₀ O	C ₄ H ₈ O ₂	CO ₂
Slope (b)	0.33±0.029	0.034±0.0004	0.04±0.004	0.010±0.004	0.012±0.001	0.005±0.001
Intercept (a)	1.12±0.058	0.86±0.014	0.26±0.022	1.145±0.018	2.057±0.018	3.69±0.020
R ²	0.9750	0.9874	0.9950	0.9934	0.9798	0.9947
LOD (ppm)	1.55	2.55	2.62	48.00	46.75	15.60
LQD (ppm)	5.20	8.52	8.75	162.00	155.83	52.10
Response time t ₉₀	50	20	25	32	30	28
Recovery time t ₁₀	170	60	58	65	68	62

Table 3. A comparison of the performance of resistive sensors based on C-XTiO₂ in the detection of different gases.

Material	Synthesis	Gas	[Gas] ppm	Response time (s)	Recovery time (s)	Phase	TiO ₂ size (nm)	Sensor response	T (°C)	Ref.
C-Ti	Sol-gel	NO ₂	10	240	1044	-	8.8	R _g /R _a	Room T.	[24]
C-Ti nano composite	Sol-gel	NO ₂	1-100	-	-	p-type	-	(R ₀ -R _{gas})/R ₀ x100	50-200	[25]
C-Ti nano tubes array	Chem. Thermal.	H ₂	5000	-	-	-	-	current	100	[26]
C-xTi	Solvothermal-calc.	Pentanol	100	100	675	-	30	R _a /R _g	170	[19]
C-xTi	Sol-gel	NH ₃	0-100	50	170	n-type	-	(R _g -R _a)/R _a x100	Room T.	Current Study